Single-molecule analysis of a molecular disassemblase reveals the mechanism of Hsc70-driven clathrin uncoating

Till Böcking[1,2,5], François Aguet[2], Stephen C Harrison[3,4] & Tomas Kirchhausen[1,2]

Heat shock cognate protein-70 (Hsc70) supports remodeling of protein complexes, such as disassembly of clathrin coats on endocytic coated vesicles. To understand how a simple ATP-driven molecular clamp catalyzes a large-scale disassembly reaction, we have used single-particle fluorescence imaging to track the dynamics of Hsc70 and its clathrin substrate in real time. Hsc70 accumulates to a critical level, determined by kinetic modeling to be one Hsc70 for every two functional attachment sites; rapid, all-or-none uncoating then ensues. We propose that Hsc70 traps conformational distortions, seen previously by cryo-EM, in the vicinity of each occupied site and that accumulation of local strains destabilizes the clathrin lattice. Capture of conformational fluctuations may be a general mechanism for chaperone-driven disassembly of protein complexes.

Molecular chaperones in the heat-shock protein-70 (Hsp70) family impart directionality to a wide variety of intracellular assembly and translocation processes. For example, DnaK, one of three *Escherichia coli* Hsp70 family members, dissociates DNA-replication origin complexes[1] and accelerates protein folding[2], and BiP drives post-translational transport of secreted proteins into the endoplasmic reticulum of eukaryotic cells[3]. Hsc70, the most abundant cytosolic family member, essential for cell viability, has many distinct functions, both in preventing or reversing protein aggregation and in disassembling protein complexes[4,5]. The best characterized of the disassembly activities is its role in uncoating the clathrin lattice that surrounds an endocytic coated vesicle[6–8].

Clathrin has the form of a triskelion—a three-legged object, in which each leg comprises a 180-kDa heavy chain and a ~30-kDa light chain[9]. These trimeric assembly units associate into a lattice-like coat that promotes engulfment of a vesicle from a cellular membrane[10] (**Fig. 1** and **Supplementary Fig. 1**). When the vesicle has separated completely from the parent membrane, the coat disassembles, allowing the vesicle to dock and fuse with other vesicles or with large, membrane-delimited compartments and recycling of the coat components[11,12]. Timing of the uncoating step, so that it follows promptly upon completion of the clathrin lattice and pinching off of the enclosed membrane vesicle, is determined by arrival of auxilin, a protein with a C-terminal J-domain—a module that recruits Hsp70-family chaperones. Recognition that the vesicle contained within a clathrin coat has indeed pinched off and separated from the parent membrane is a function of the PTEN-like region at the N-terminal part of auxilin[11,12].

The structures of a clathrin coat, determined at subnanometer resolution by cryo-EM[10], and of coats with bound auxilin C-terminal region (J-domain and clathrin-binding module)[13] and with bound Hsc70 (ref. 14) lead to the following picture for steps in the uncoating process. Like all Hsp70 family members, Hsc70 is an ATP-driven molecular clamp

with an ATPase domain and a substrate-binding domain. Recruited to the vicinity of a target peptide by a J-domain protein, Hsc70–ATP binds the peptide in a groove on its substrate-binding domain. ATP hydrolysis, stimulated by encounter with the target and the J-domain, clamps the groove in the closed state and releases the J-domain contact. Exchange of ATP for ADP reopens the groove, liberates the substrate and resets the cycle. The peptide groove accommodates about five to seven amino acid residues, with a preference for hydrophobic residues and a particular preference for the sequence FYQLALT[15]. The closely related QLMLT sequence near the C terminus of a clathrin heavy chain is the site required for Hsc70-driven uncoating[16]. The three such sites on a clathrin trimer are exposed beneath each vertex of a coat within a narrow, inward-opening funnel formed by the crisscrossing 'ankle' segments of three other clathrin trimers (**Fig. 1**). Auxilin binding, which brings up to three J-domains into the neighborhood of each vertex, favors local displacements of the ankle segments, leading to expansion of the funnel and allowing Hsc70 to access its target segment. Even the displaced ankle segments probably leave only enough space to admit a single Hsc70. ATP hydrolysis clamps this Hsc70 in place and locks the locally distorted configuration. This structural description has led to the proposal that accumulation of a sufficient number of such distorted configurations destabilizes the lattice and initiates disassembly. In the work reported here, we have tested this proposal by using sensitive single-particle fluorescence experiments with high time resolution to follow the HSC70- and auxilin-dependent disassembly of clathrin coats.

RESULTS

Single-particle fluorescence imaging of clathrin coats

In the uncoating process suggested by the cryo-EM structures, Hsc70 destabilizes a coat by trapping local excursions from an equilibrium

[1]Immune Disease Institute, Harvard Medical School, Boston, Massachusetts, USA. [2]Department of Cell Biology, Harvard Medical School, Boston, Massachusetts, USA. [3]Department of Biological Chemistry and Molecular Pharmacology, Harvard Medical School, Boston, Massachusetts, USA. [4]Howard Hughes Medical Institute, Harvard Medical School, Boston, Massachusetts, USA. [5]Centre for Vascular Research, University of New South Wales, Australia. Correspondence should be addressed to T.K. (kirchhausen@crystal.harvard.edu).

Figure 1 A clathrin coat with views of a vertex before and after formation of an uncoating intermediate. (**a**) Schematic representation of clathrin triskelions in a D6-barrel lattice (PDB 1XI4; ref. 10). One clathrin triskelion is highlighted in blue. The green shaded leg segments show the invariant contact between proximal (p) and distal (d) legs of the triskelions indicated by green asterisks at their hubs. The green arrow shows the direction of conformational shift when auxilin and Hsc70 bind. The hook-like elements at the (N-terminal) tips of the legs represent the β-propeller terminal domains. (**b**) Detail of a vertex before binding of auxilin


and Hsc70. The unstructured C termini of the clathrin heavy chain (blue balls), which contain the Q_{1638}LMLT Hsc70-binding motif (narrow orange arrows), extend inward from the helical tripod at the triskelion hub[14]. The ankle (a) and terminal domain (t) shift in the direction of the wide green arrow when auxilin and Hsc70 bind. (**c**) Relative locations of bound auxilin (red spheres) and Hsc70 (orange lozenge) as determined by cryo-EM[13,14]. The shift in the positions of the clathrin ankle and terminal domain have been exaggerated to illustrate the expansion of the funnel surrounding the Hsc70-binding motif.
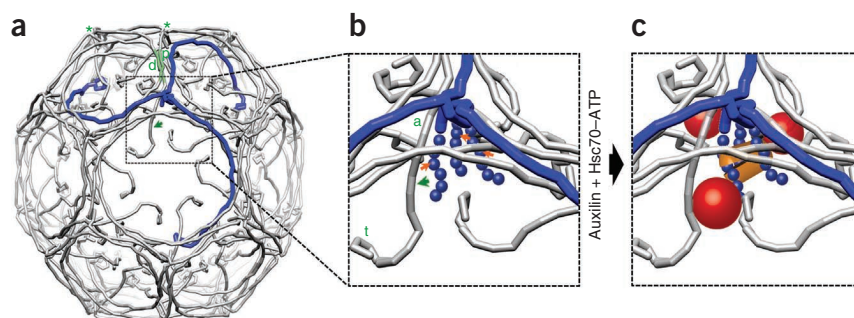
conformation—a specific example of a general class of disassembly mechanisms. To distinguish between this kind of model and ones in which Hsc70 has a directly 'mechanical' role, we have designed a single-particle fluorescence imaging assay in which we visualize directly the Hsc70 driven disassembly of clathrin coats (**Fig. 2**). We prepared fluorescent coats from recombinant clathrin trimers, site-specifically labeled at Cys187 of the light chains with Alexa Fluor 488 (AF488) (**Supplementary Fig. 1**). These coats, assembled with the AP-2 heterotetrameric adaptor complex as in our previous work[10], had the same D6-barrel morphology (36 clathrin triskelions) and the same bulk uncoating behavior as coats assembled from unlabeled clathrin[16] (**Supplementary Fig. 2**). Coats were captured

by the monoclonal antibody CVC.6, to clathrin light chain a1 (LCa) (ref. 17), on the surface of a coverslip modified with an inert layer of PEG to prevent nonspecific adsorption of fluorescent proteins and collapse of the clathrin coat through strong interaction with the glass surface[18] (**Supplementary Fig. 3**). The coverslip forms the bottom of a microfluidic flow cell fabricated in polydimethylsiloxane for delivery of uncoating reagents (**Supplementary Fig. 4**). After binding of auxilin to the captured coats, we introduced a solution containing auxilin, ATP and Hsc70 C-terminally tagged with Alexa Fluor 568 (AF568) (**Supplementary Fig. 5**), while monitoring the fluorescence intensities of clathrin and Hsc70 at each location in the field of view that corresponded to a single coat (**Fig. 2a**).

Figure 2 Single-particle visualization of clathrin uncoating. (**a**) Schematic representation of the single-particle uncoating assay. The intensities of fluorescence from labeled clathrin and Hsc70 were monitored by TIRF microscopy for clathrin–AP-2 coats captured on the surface of a PEG-modified glass coverslip. (**b**) Representative time series of a single-particle uncoating assay. Left and right panels, first and last frames, respectively, of the fluorescence channel used to monitor the signal from coats tagged with clathrin LCa–AF488. Middle, kymograph generated from the vertical axis indicated by the arrows in the left panel, showing the unsynchronized disappearance of clathrin fluorescence. Hsc70–ATP (1.2 μM) arrived in the flow chamber at $t = 0$. (**c**) Uncoating profile from a single coat. The selected snapshots from the time series (top) show the fluorescence from clathrin and Hsc70 in the selected coat, at various time points during the uncoating reaction carried out with 0.9 μM Hsc70. The snapshots are background-corrected averages of three successive frames. The plot shows intensity traces of the clathrin (blue) and Hsc70 (orange) signals. The $t = 0$ time point is the moment at which a rapid increase in Hsc70 background signal is recorded; this event corresponds to the arrival of Hsc70 within the evanescent field at the coverslip. (**d**) Histogram of the number of trimers (triskelions) per coat at the beginning (top) and the end (bottom)

of the single-particle uncoating assay carried out with 1.2 μM Hsc70. The number of trimers in intact coats follows a normal distribution with a mean of 34 triskelions per coat (top). In most cases, only one or two trimers remained at the site of a coat at the end of the reaction (bottom). Objects with overlapping point-spread functions were excluded from this analysis. A.u., arbitrary units.
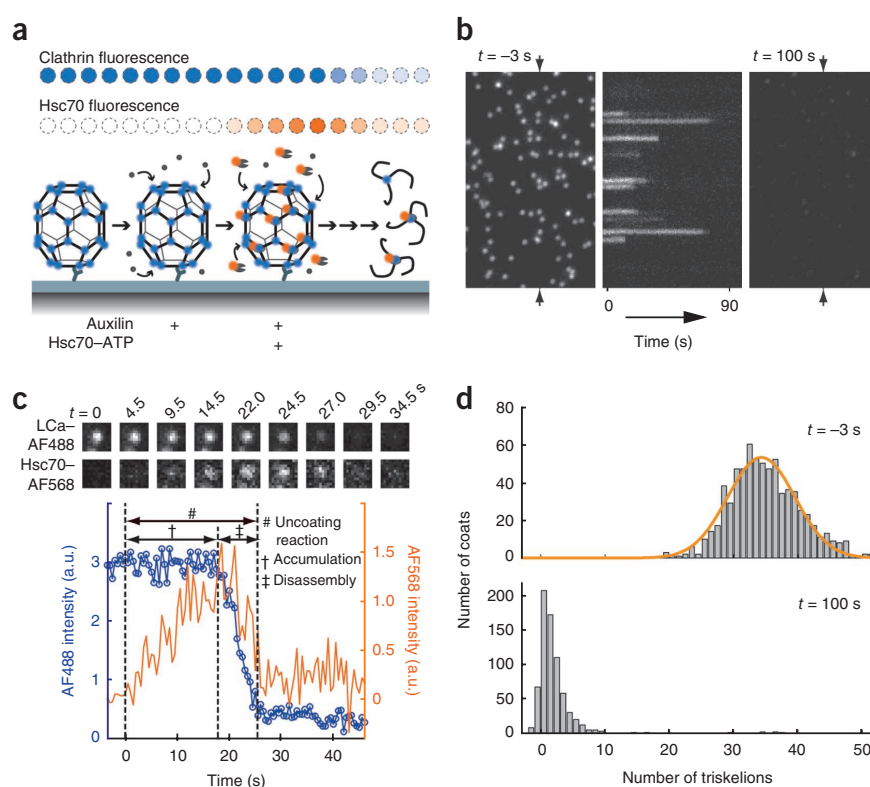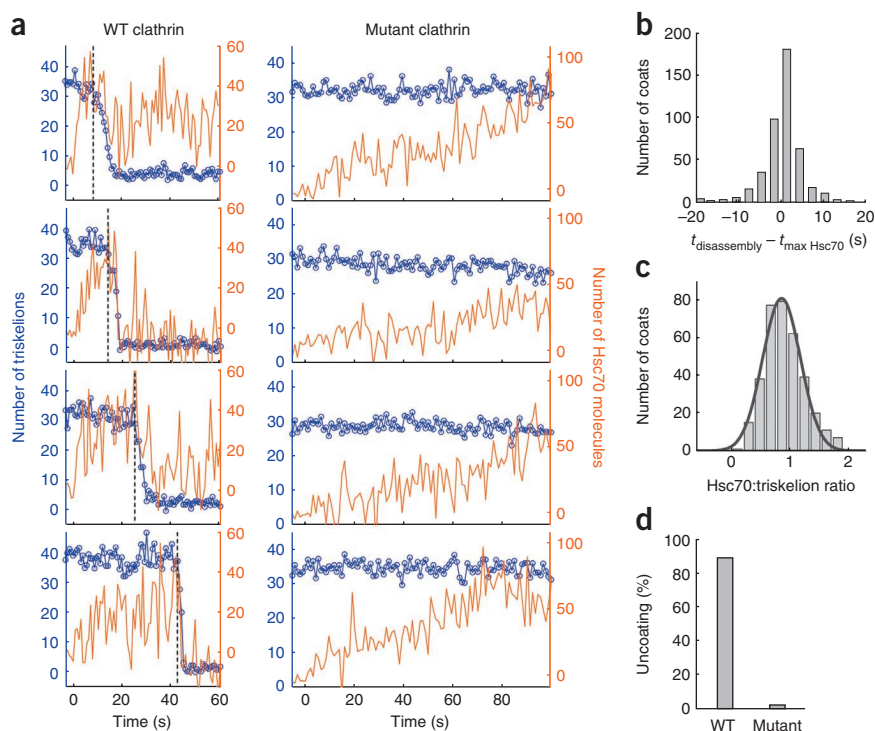
Figure 3 Requirement of the Hsc70 binding motif for Hsc70-driven uncoating. (**a**) Representative uncoating traces for clathrin–AP-2 coats assembled with wild-type (WT) heavy chain clathrin (left panels) or mutant heavy chain clathrin truncated at its C terminus to remove the Hsc70 binding site (right panels). Hsc70–ATP (1.2 µM) arrived at $t = 0$ during monitoring of the fluorescence intensities of clathrin (blue) and Hsc70 (orange) with TIRF illumination. Vertical dotted lines indicate onset of coat disassembly. The Hsc70:triskelion ratios at the onset of coat disassembly for the WT traces are 1.0, 0.8, 1.2 and 0.6, from top to bottom. (**b**) Histogram of the time difference between maximal Hsc70 binding and onset of coat disassembly. (**c**) Histogram of the number of Hsc70 molecules bound per triskelion determined from the ratio of calibrated fluorescence intensities of Hsc70 to clathrin at the onset of coat disassembly (0.9 ± 0.3, $N = 350$ coats). See Online Methods for details. (**d**) Uncoating efficiency for coats assembled with either WT ($N = 582$ coats) or mutant clathrin ($N = 660$).

When imaged by total internal reflection fluorescence (TIRF) microscopy, the fluorophore-tagged coats ~75 nm in diameter appeared as diffraction limited spots of similar intensities (**Fig. 2b,d**). The coats were stable for an extended time (half-life of coat intensity, ~2 h) in the absence of free clathrin and uncoating reagents. After injection of the uncoating solution, rapid dissociation of most coats followed an 'accumulation period' for Hsc70 binding that depended on Hsc70 concentration (**Fig. 2c**). The individual disassembly events reported by the intensity decay were not synchronous, and coats began to dissociate at different times after introduction of the uncoating mixture (kymograph in **Fig. 2b**). At the end of the experiment, there was a residual signal at each coat location, corresponding to the one (or a few) clathrin trimers bound to the surface-immobilized antibody (**Fig. 2d**). This residual clathrin also retained, on average, about three Hsc70 molecules per trimer (**Supplementary Fig. 6**).

To determine the ensemble behavior, we calculated the mean fluorescence intensity of all coats in the field of view and found a single exponential decrease (half-life, ~6 s for 2 µM Hsc70; **Supplementary Fig. 7**), recapitulating the data from bulk experiments that monitor the decrease in light scattering from solutions of coats to which auxilin, Hsc70 and ATP have been added[19,20]. We conclude that the traces from immobilized coats in our experiments faithfully represent the ensemble behavior of comparable coats in solution.

Kinetics of disassembly mediated by Hsc70–ATP and auxilin

Analyses of single-particle uncoating kinetics yield far more detailed mechanistic information than do ensemble measurements. In particular, our single-particle assay provides data for determining parameters of a realistic kinetic scheme and for distinguishing among alternative mechanisms. In a typical experiment, we tracked the real-time dissociation kinetics of several hundred individual AF488-labeled coats (**Supplementary Fig. 8**) with prebound auxilin$_{547-910}$, a fragment sufficient to direct uncoating[8,13,16]. We introduced AF568–labeled Hsc70, and taking its appearance in the evanescent field as $t = 0$, we obtained Hsc70 binding and clathrin uncoating traces from fits of

Gaussian-approximated point spread functions to the corresponding signals (**Figs. 2c** and **3a** and **Supplementary Fig. 8b**). During a characteristic accumulation period, the Hsc70 signal increased steadily while the clathrin signal remained constant. When the Hsc70 signal reached a critical level, both signals began to decrease together and decayed rapidly to close to background (**Fig. 3a,b**). Most traces showed a rapid disassembly phase (for rarer classes of behavior at the single-particle level, see **Supplementary Fig. 8**). In some instances, decay of the Hsc70 signal lagged loss of the clathrin signal (**Fig. 3b**), indicating additional association of Hsc70 at unoccupied binding sites in the coat during the disassembly phase. Calibration of the intensity traces with data from single-molecule measurements (see **Fig. 3c** and **Supplementary Figs. 1** and **5**) yielded a ratio of about one Hsc70 per clathrin trimer, but because this ratio includes specific and nonspecific binding of Hsc70, it is an upper limit for the amount of Hsc70 required to initiate uncoating (see below). We define "specific binding" as productive association of Hsc70 at the QLMLT motif, shown in our earlier work[16] to be required for Hsc70-dependent uncoating, and "nonspecific binding" as unproductive association of Hsc70 at other sites in the coat.
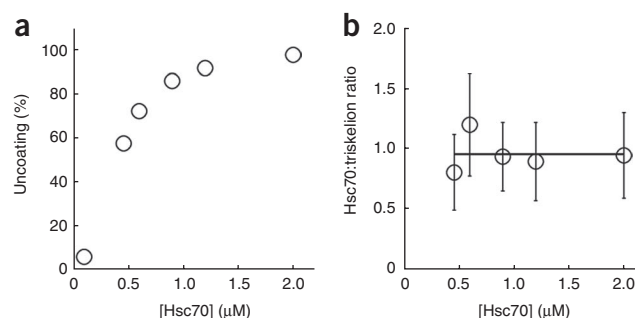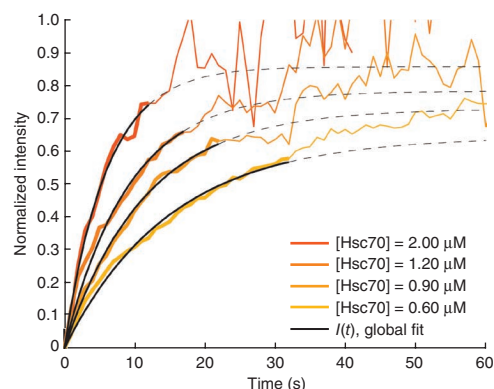

Figure 4 Hsc70 concentration dependence of the uncoating reaction. (**a**) Uncoating efficiency as a function of Hsc70 concentration. (**b**) Number of Hsc70 molecules bound per triskelion (mean ± s.d.) as a function of Hsc70 concentration determined from the ratio of the Hsc70 to the clathrin fluorescence intensity at the transition point between the accumulation and disassembly stages.

Figure 5 Recruitment of Hsc70 to clathrin–AP-2 coats during the accumulation phase follows first-order kinetics. The colored traces correspond to the averaged intensity of the Hsc70 fluorescence measurements recorded in separate, single-particle uncoating assays with various Hsc70 concentrations. We used a global fit of the accumulation phase up to the mean accumulation time for each concentration (black line) to determine the association and dissociation rates of Hsc70 binding. Mean accumulation times are derived from the accumulation time distributions in **Figure 6**. During this early recruitment phase, Hsc70 binds preferentially to the QLMLT sequence after activation by the neighboring auxilin J-domain. During the later stages, when most of the specific sites have been occupied, activated Hsc70 is presumably delivered to other sites, which do not drive disassembly. The average Hsc70 binding curves become noisy beyond their corresponding mean accumulation times because most coats have started to disassemble, and the average is calculated from an increasingly lower number of coats. The dashed lines show the binding curves from the calculated parameters, beyond the range of the data used for fitting.

Clathrin coats assembled from heavy chain C-terminal truncation mutants lacking the Hsc70 binding motif showed slow, nonproductive Hsc70 binding that did not result in coat disassembly (**Fig. 3a,d**). Uncoating also did not occur in the absence of ATP or auxilin (**Supplementary Fig. 9**). Under the latter conditions, nonspecific binding was also greatly reduced, as in previous studies of Hsp70-family chaperones[21].

We investigated the uncoating reaction at Hsc70 concentrations ranging from 0.1 to 2 µM. Typical intracellular concentrations are 20–30 µM (ref. 22). The frequency of uncoating events decreased with decreasing Hsc70 concentration, and at the lowest concentrations we studied, only a fraction of the coats disassembled even after 5 min (**Fig. 4a**). Disassembly, when it occurred, was nearly always complete, and only in very rare cases did we observe partial uncoating. The amount of residual clathrin remaining on the surface at the end of a typical uncoating experiment was ≤1 triskelion for 40% of the coats, ≤3 triskelions for 80% of the coats and ≤6 triskelions for 95% of the coats (**Fig. 2d**). Inspection of individual traces at various Hsc70 concentrations showed that the amount of Hsc70 accumulation was roughly uniform and relatively independent of concentration in the subset of coats that disassembled (**Fig. 4b**), but lower and more variable in those coats that did not come apart.

Kinetic model for Hsc70-driven uncoating

Analysis of the Hsc70 recruitment signal through numerical fitting of a binding equation at various Hsc70 concentrations yields the rate constants $k_1^+ = {\sim}0.070\ \mu M^{-1}\ s^{-1}$ and $k_1^- = {\sim}0.027\ s^{-1}$ (**Fig. 5**). A single

value for k_1^+ fits the data at various concentrations and at various times during the association phase, indicating that binding at a vertex is noncooperative (at least during the observable phase of recruitment) and also independent of nonspecific binding (**Fig. 5**). On the basis of these rates, we analyzed the accumulation-time distributions (**Fig. 6**, pink) and the time distributions for the entire uncoating reaction (**Fig. 6**, blue) using the kinetic scheme depicted in **Figure 6a**. The accumulation time corresponds to the first phase of the uncoating reaction: binding of Hsc70 to the intact coat; it is the time during which the clathrin signal remains relatively constant (**Fig. 2c**). The entire uncoating reaction time includes both accumulation and disassembly phases; it extends from the initial appearance of an Hsc70 fluorescent signal to the time at which the clathrin fluorescent signal
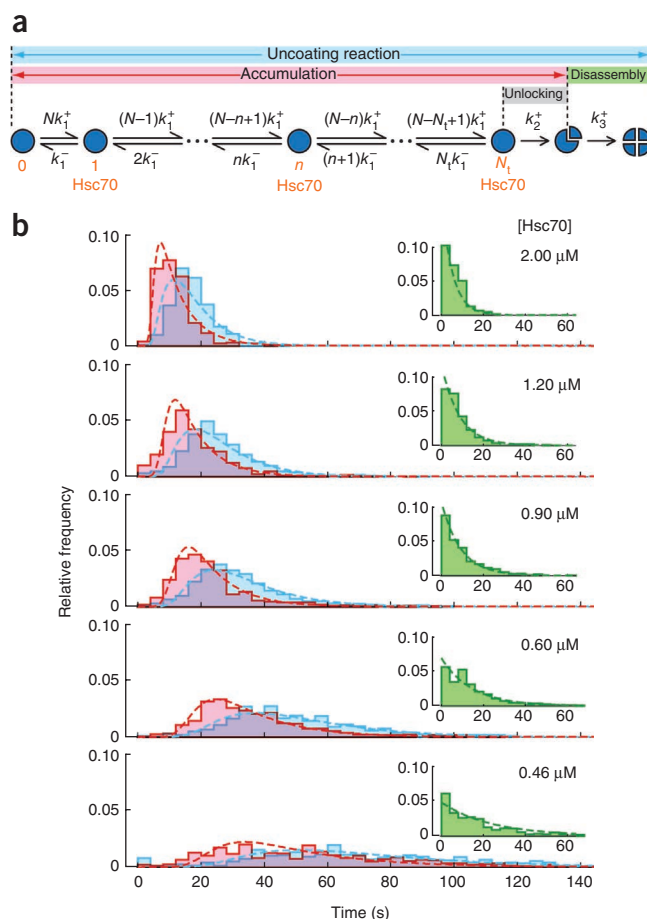
Figure 6 Kinetic model for the uncoating reaction. (**a**) Scheme for the kinetic analysis of Hsc70-driven uncoating. The model assumes that a threshold number of sites in the coat, N_t, must be occupied by a productively bound Hsc70 molecule to initiate disassembly. Hsc70 binds independently to the N binding positions in the coat ($N = 36$ for the D6 barrel), with a microscopic association rate constant k_1^+ (determined from the Hsc70 association curves; see **Supplementary Methods** and **Fig. 5**). The rate of any step is given by the product of k_1^+ and the number of unoccupied sites. Bound Hsc70 dissociates from the coat with an off-rate given by the microscopic dissociation rate constant k_1^- and the number of bound Hsc70 molecules. Binding of N_t Hsc70 molecules triggers disassembly in a single, rate-limiting step of rate constant k_2^+ (determined independently; see **Fig. 7**). The rate of clathrin dissociation, which depends linearly on Hsc70 concentration, is modeled with a single rate constant, k_3^+. (**b**) Distributions of the Hsc70 accumulation time (pink) and the full uncoating time (cyan), comprising accumulation and disassembly phases, at various Hsc70 concentrations, overlaid with fits of the kinetic model. The insets show disassembly time distributions (green) at various Hsc70 concentrations and the corresponding single exponential phase derived from the model fit.

Figure 7 Transition of Hsc70-loaded coats to the disassembly phase. (**a**) Experimental design used for the pH shift experiment. After immobilization of the clathrin–AP-2 coats on the modified coverslip, the microfluidic chamber was perfused sequentially with auxilin and then with a mixture of auxilin and Hsc70–AF568–ATP at pH 6. At this pH, the coats do not dissociate[23]. To trigger uncoating, the pH was shifted to 6.8 in the presence of unlabeled Hsc70–ATP. Minimal uncoating was observed if the pH shift was done in the absence of Hsc70–

ATP. (**b**) Histogram of the dwell times between pH shift and initiation of disassembly. The distribution of dwell times is a single exponential, indicating that the transition of an Hsc70-loaded coat to the disassembly phase has a single rate-limiting step, with rate constant $k_2^+ = 0.16$ s^{-1}.
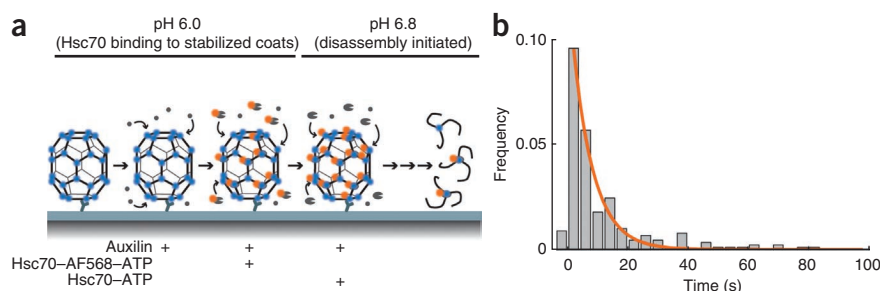
has decayed to a stable, residual level (**Fig. 2c**). In our model for the accumulation phase, we assumed that a single association rate constant, k_1^+, characterizes binding at any vertex and that a single dissociation rate constant, k_1^-, characterizes loss of Hsc70 from any vertex. We further assumed that when a critical number, N_t, of Hsc70 molecules are bound, a transition to the disassembly phase occurs. This 'unlocking' step, with rate constant, k_2^+, leads to initial loss of one or more clathrin trimers and commits the coat to full disassembly (**Fig. 7**). We assumed a single, additional rate constant, k_3^+, for the disassembly phase (**Fig. 6b**, insets).

The model for the accumulation phase gives the probability that after a time t a coat will start to disassemble; we used the probability distribution to determine N_t and k_2^+. A numerical fit of the rate equations to the accumulation time distributions (**Fig. 6b**, pink) showed that uncoating is triggered when Hsc70 has accumulated to about 1 molecule for every 2 triskelions—that is, we find $N_t \approx 18$ for all Hsc70 concentrations (**Supplementary Fig. 10**). Details of the kinetic analysis are provided in the **Supplementary Methods**. The difference between this estimate and the value of about 1 per vertex, obtained from the ratio of Hsc70 and clathrin fluorescence signals at the time of disassembly (**Fig. 4b**), is probably due to nonspecific binding at sites other than the effective one beneath the triskelion hub. We show below that auxilin can recruit Hsc70 and deliver it to nonspecific sites as well as to the functional QLMLT segment. Hsc70 at these sites contributes to the estimate of N_t from intensity ratios, but does not contribute to the estimate from the kinetic model. Binding of Hsc70 to unoccupied sites can also continue throughout the transition (unlocking) and disassembly steps after loading with N_t Hsc70 molecules has triggered uncoating. Thus, the cumulative number of bound Hsc70, as determined biochemically for saturation of Hsc70 on coats at low pH[8,14] or for clathrin trimers released from the coat[20] is necessarily higher than N_t.

We have also derived a direct measurement of the rate constant, k_2^+, associated with the penultimate step in the kinetic scheme (commitment to uncoating), from an independent experiment in which we added fluorophore-labeled Hsc70 to coats at pH 6 (**Fig. 7**). The lowered pH stabilizes the coat[23], allowing Hsc70 to accumulate to roughly 1 molecule per triskelion. We then rapidly raised the pH to 6.8, in the presence of unlabeled Hsc70 and ATP, and followed the ensuing disassembly. Coats that disassembled promptly had lost little of their tagged Hsc70 at the onset of uncoating. (For a discussion of Hsc70 exchange, see **Supplementary Methods**.) We could fit the exponential delay-time distribution for entry of these coats into the disassembly phase with a first-order rate constant, $k_2^+ = 0.16$ s^{-1}, essentially equal to the value we obtained from analysis of the uncoating experiments in **Figure 6**, which were carried out at constant pH. This experiment also shows that the low-pH-stabilized,

Hsc70-bound coat structure that we determined by cryo-EM[14] indeed represents an on-pathway or near-pathway intermediate, and not an off-pathway dead end.

We used two approaches to estimate the rate constant governing the disassembly phase, allowing us to extend the model to cover the entire uncoating reaction. Distributions of the disassembly times, defined as the times between start and end of the decay in the clathrin signal, revealed a single rate-limiting step (single exponential decay) that depended linearly on Hsc70 concentration (**Fig. 6b**, insets, green; **Supplementary Fig. 11**). A global fit of the uncoating reaction time distributions with the full model including this final step yielded an estimate for the rate constant of $k_3^+ = 0.105$ μM^{-1} s^{-1} (**Fig. 6b**, blue; **Supplementary Fig. 11**). The concentration dependence of the disassembly rate shows that Hsc70 loading must be maintained to sustain disassembly. Indeed, coats stopped dissociating if all bound Hsc70 was lost during the disassembly phase. In cells, uncoating is rapid and does not stall, because the cytosolic concentration of Hsc70 (20–30 μM), much higher than the concentrations used here, is greater than the overall K_d for the uncoating reaction.

Mixed coats

If Hsc70 must accumulate to a ratio of at least 1:2 Hsc70:clathrin triskelion before disassembly can begin, then coats doped with clathrin lacking the Q_{1638}LMLT Hsc70-binding motif should resist uncoating, to an extent that depends on the amount of mutant clathrin in the lattice. We assembled coats with varying ratios of wild-type clathrin to mutant clathrin truncated at residue 1637, labeled respectively with LCa–AF488 and LCa–DyLight 649 (DL649). We then mixed the assembly products, captured the mixture with CVC.6 and analyzed uncoating with 1.26 μM Hsc70. We determined the ratio of wild-type to mutant clathrin in any individual coat from the ratio of their fluorophores and followed Hsc70 accumulation by monitoring a third fluorophore (AF568) (**Fig. 8**; see also **Supplementary Fig. 12**). The coat with a 20:80 ratio of wild-type:mutant clathrin did not disassemble (**Fig. 8b**); the one with a 80:20 ratio did (**Fig. 8c**), with simultaneous release of both species. That is, there was no selective release of wild-type or mutant clathrin, even from those coats with a small enough doping of mutant clathrin that uncoating eventually occurred. **Figure 8d** shows the fraction of coats that disassembled rapidly, as a function of their wild-type clathrin content. These observations rule out a model in which binding of Hsc70 to an individual triskelion results directly in its removal from a coat. There was continuous accumulation of Hsc70 on a coat that could not disassemble and that contained 80% truncated clathrin (**Fig. 8c**). Total accumulation during the relatively long incubation (>1 min) exceeded 2 Hsc70 molecules per triskelion, showing that most of the bound Hsc70 was
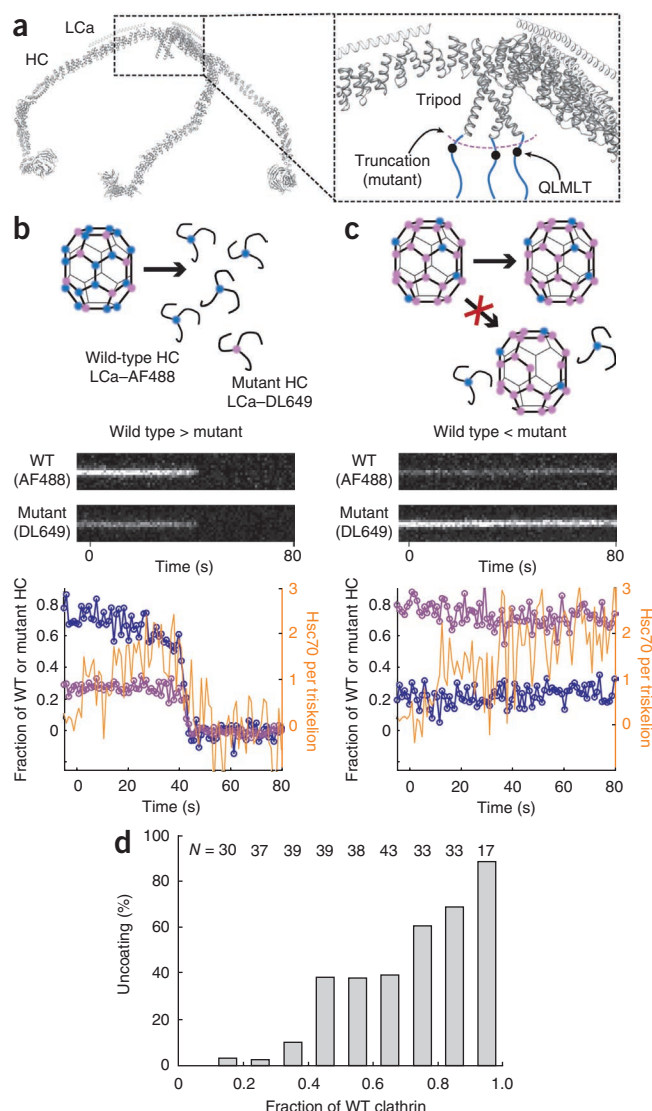
Figure 8 Uncoating reaction with coats containing mixtures of wild-type and mutant clathrin. (**a**) Backbone model of the heavy and light chains of a clathrin triskelion (PDB 3IYV)[10]. The close-up of a triskelion hub shows the location of the binding site for Hsc70 (QLMLT motif, black dots) in the C-terminal unstructured region of the clathrin heavy chain (HC; blue lines). (**b,c**) Outcome of the uncoating reaction for coats containing mostly wild-type (WT) (**b**) or mostly mutant clathrin lacking the Hsc70-binding motif (**c**). Coats containing primarily WT clathrin underwent normal disassembly with release of WT and mutant clathrin (left); coats containing primarily mutant clathrin remained intact, and no WT clathrin was released. Top, schematic representation of the coats and the outcome of the uncoating reaction. Middle, representative kymographs of single-particle uncoating traces from two coats, one containing excess WT clathrin (80%, left) and the other containing excess mutant clathrin (80%, right); WT and mutant clathrin were labeled with LCa–AF488 and LCa–DL649, respectively. Bottom, plots of fluorescence intensity traces: blue, WT clathrin; purple, mutant clathrin; orange, Hsc70. (**d**) Uncoating efficiency as a function of the fraction of WT clathrin in the coat. Coats with different ratios of WT and mutant clathrin were prepared and mixed; their disassembly properties were then analyzed together in the same field (*N* = 311 coats).

Can we correlate these observations with the known structural features of the Hsc70-bound coat, to derive a molecular description of the Hsc70-driven uncoating mechanism? The structure of an Hsc70-containing coat suggests that binding of Hsc70 to its preferred site near the C terminus of a heavy chain will not destabilize the triskelion to which it clamps but rather each of the three triskelions contributing heavy-chain ankle segments to the funnel-like cavity into which Hsc70 inserts. These ankle segments must shift to make room for Hsc70—that is, Hsc70 binding and ATP hydrolysis capture a local perturbation. The ankles belong to triskelions centered two vertices away, and they connect into distal leg segments, part of the invariant interface that provides favorable interaction free energy for coat assembly (**Fig. 1b**, green arrowheads). In the low-pH stabilized form examined by cryo-EM, these invariant interfaces are fixed, and the perturbation that has allowed Hsc70 to access its site does not propagate beyond the ankle. But at neutral pH, it is likely that a conformational fluctuation away from optimal registration of the invariant interface will relieve some of the strain on the ankle, increasing the lifetime of the altered conformation and hence increasing the probability that it will coincide with a similar fluctuation in another leg of the same triskelion.

As an example, suppose that the first triskelion to dissociate will tend to leave the coat when interactions of at least two of its ankle segments and their contiguous distal-leg segments have been destabilized. Then a transition to the uncoating phase will become likely when Hsc70 occupies over half the vertices. Once uncoating has commenced, however, loss of triskelions (or groups of triskelions) will continue, as reassociation of clathrin is hindered by Hsc70 still in place at many remaining vertices. Clathrin trimers at the edge of a disassembling coat will be ejected by a destabilizing Hsc70 at their ankles and by the absence of contacts from molecules already lost. In our experiments, there is no free clathrin to refill vacancies, except the small amount released by uncoating. In the cell, there is a cytosolic pool of free clathrin that could, in principle, reverse the uncoating, were the vertices of the dissociating lattice not blocked by Hsc70. In practice, extra mechanisms contribute to triskelion recruitment by a growing clathrin lattice on the plasma membrane, so that regrowth of a coat on a pinched-off vesicle would be unlikely even were Hsc70 not in place.

In the mechanism we propose, Hsc70 traps a conformational fluctuation at one vertex for long enough that more fluctuations at other vertices can reinforce each other in destabilizing the coat. ATP

at sites other than the one at position 1638, which was missing from all but 20% of the heavy chains. This nonspecific background binding was much lower in the absence of auxilin (**Supplementary Fig. 9**). That is, when the wild type–specific site has been deleted, the auxilin J domain seems to recruit Hsc70 and to deliver it to distributed sites on the coat that do not drive disassembly.

DISCUSSION

Measurement of single-particle kinetics has allowed us to make distinctions about the order of molecular events that we could not determine from ensemble measurements. In particular, the distribution of accumulation times in bulk solution and hence the dephasing of individual disassembly reactions, even if initiated by rapid addition of Hsc70, would obscure the following important characteristics of clathrin uncoating. (i) Uncoating is an all-or-none process: either a coat disassembles completely or does not disassemble at all. Nonetheless, uncoating requires the continued presence of bound Hsc70. (ii) Roughly 0.5 Hsc70 molecules per clathrin trimer must accumulate on average, under the conditions of our experiments, before uncoating can begin. (iii) Binding of Hsc70 at one vertex is, in first approximation, independent of binding at other vertices. (iv) Dissociation of a clathrin trimer does not depend on its contact with an Hsc70 molecule but only on whether its coat is disassembling.

hydrolysis is obviously essential for unidirectionality. Also critical for this mechanism are the sequence and location of the specific Hsc70 site. Scrambling of the target sequence eliminates Hsc70-driven uncoating[16], as does the truncation used in the experiments reported here. That is, Hsc70 binding elsewhere on the coat does not promote disassembly. Moreover, the position and orientation of the auxilin J-domain within the lattice allows preferential delivery of Hsc70 to the QLMLT segment, during its transient exposure. In principle, any intracellular assembly could acquire a comparable pathway for regulated dissociation by evolving a J-protein recruitment mechanism and a preferred Hsc70 recognition site in a location that allows chaperone binding to trap a destabilizing conformational fluctuation. We propose these characteristics as a general description of how Hsp70-family chaperones take apart large protein complexes.

METHODS
Methods and any associated references are available in the online version of the paper at http://www.nature.com/nsmb/.

Note: Supplementary information is available on the Nature Structural & Molecular Biology website.

AUTHOR CONTRIBUTIONS
T.B. and T.K. developed the single-molecule assay and T.B. performed experiments; T.B. and F.A. analyzed data; F.A. developed the kinetic model. T.B., S.C.H. and T.K. designed experiments. All authors discussed the results and contributed to the final manuscript.

COMPETING FINANCIAL INTERESTS
The authors declare no competing financial interests.

Published online at http://www.nature.com/nsmb/.
Reprints and permissions information is available online at http://npg.nature.com/reprintsandpermissions/.

1. Dodson, M., McMacken, R. & Echols, H. Specialized nucleoprotein structures at the origin of replication of bacteriophage lambda. Protein association and disassociation reactions responsible for localized initiation of replication. *J. Biol. Chem.* **264**, 10719–10725 (1989).
2. Hartl, F.U. & Hayer-Hartl, M. Converging concepts of protein folding *in vitro* and *in vivo*. *Nat. Struct. Mol. Biol.* **16**, 574–581 (2009).
3. Rapoport, T.A. Protein translocation across the eukaryotic endoplasmic reticulum and bacterial plasma membranes. *Nature* **450**, 663–669 (2007).
4. Mayer, M.P. & Bukau, B. Hsp70 chaperones: cellular functions and molecular mechanism. *Cell. Mol. Life Sci.* **62**, 670–684 (2005).
5. Young, J.C., Barral, J.M. & Ulrich Hartl, F. More than folding: localized functions of cytosolic chaperones. *Trends Biochem. Sci.* **28**, 541–547 (2003).
6. Schlossman, D.M., Schmid, S.L., Braell, W.A. & Rothman, J.E. An enzyme that removes clathrin coats: purification of an uncoating ATPase. *J. Cell Biol.* **99**, 723–733 (1984).
7. Greene, L.E. & Eisenberg, E. Dissociation of clathrin from coated vesicles by the uncoating ATPase. *J. Biol. Chem.* **265**, 6682–6687 (1990).
8. Ungewickell, E. *et al.* Role of auxilin in uncoating clathrin-coated vesicles. *Nature* **378**, 632–635 (1995).
9. Kirchhausen, T. Clathrin. *Annu. Rev. Biochem.* **69**, 699–727 (2000).
10. Fotin, A. *et al.* Molecular model for a complete clathrin lattice from electron cryomicroscopy. *Nature* **432**, 573–579 (2004).
11. Lee, D.W., Wu, X., Eisenberg, E. & Greene, L.E. Recruitment dynamics of GAK and auxilin to clathrin-coated pits during endocytosis. *J. Cell Sci.* **119**, 3502–3512 (2006).
12. Massol, R.H., Boll, W., Griffin, A.M. & Kirchhausen, T. A burst of auxilin recruitment determines the onset of clathrin-coated vesicle uncoating. *Proc. Natl. Acad. Sci. USA* **103**, 10265–10270 (2006).
13. Fotin, A. *et al.* Structure of an auxilin-bound clathrin coat and its implications for the mechanism of uncoating. *Nature* **432**, 649–653 (2004).
14. Xing, Y. *et al.* Structure of clathrin coat with bound Hsc70 and auxilin: mechanism of Hsc70-facilitated disassembly. *EMBO J.* **29**, 655–665 (2010).
15. Fourie, A.M., Sambrook, J.F. & Gething, M.J. Common and divergent peptide binding specificities of hsp70 molecular chaperones. *J. Biol. Chem.* **269**, 30470–30478 (1994).
16. Rapoport, I., Boll, W., Yu, A., Böcking, T. & Kirchhausen, T. A motif in the clathrin heavy chain required for the Hsc70/auxilin uncoating reaction. *Mol. Biol. Cell* **19**, 405–413 (2008).
17. Kirchhausen, T., Harrison, S.C., Parham, P. & Brodsky, F.M. Location and distribution of the light chains in clathrin trimers. *Proc. Natl. Acad. Sci. USA* **80**, 2481–2485 (1983).
18. Ehrlich, M. *et al.* Endocytosis by random initiation and stabilization of clathrin-coated pits. *Cell* **118**, 591–605 (2004).
19. Jiang, J., Prasad, K., Lafer, E.M. & Sousa, R. Structural basis of interdomain communication in the Hsc70 chaperone. *Mol. Cell* **20**, 513–524 (2005).
20. Schuermann, J.P. *et al.* Structure of the Hsp110:Hsc70 nucleotide exchange machine. *Mol. Cell* **31**, 232–243 (2008).
21. Misselwitz, B., Staeck, O. & Rapoport, T.A. J proteins catalytically activate Hsp70 molecules to trap a wide range of peptide sequences. *Mol. Cell* **2**, 593–603 (1998).
22. Terada, K., Kanazawa, M., Bukau, B. & Mori, M. The human DnaJ homologue dj2 facilitates mitochondrial protein import and luciferase refolding. *J. Cell Biol.* **139**, 1089–1095 (1997).
23. Barouch, W., Prasad, K., Greene, L. & Eisenberg, E. Auxilin-induced interaction of the molecular chaperone Hsc70 with clathrin baskets. *Biochemistry* **36**, 4303–4308 (1997).

ONLINE METHODS

Proteins. Wild-type rat clathrin heavy chain and a mutant truncated at residue 1637 (and hence lacking the Hsc70-binding motif 1638-QLMLT-1642) were expressed in insect cells and purified as described[16]. Rat clathrin light chain a1 (LCa) containing the mutations D203E (to restore the epitope recognized by the antibody CVC.6 (ref. 24)) and C218S (to remove one of the two cysteines in the light-chain sequence) was expressed in *E. coli* and purified as described[16]. Cys187 of LCa was reacted with an excess of a maleimide-functionalized fluorophore (AF488 or DyLight 649). The free dye was removed by ultrafiltration and the labeled LCa was purified by anion exchange chromatography. To reconstitute fluorescent clathrin, heavy-chain trimers were incubated with labeled LCa at a molar ratio of 1:2.4 for 40 min at 24 °C. UV-visible absorption spectroscopy showed that >90% of heavy chains were occupied with a labeled LCa.

The C-terminal fragment of bovine auxilin (residues 547–910) containing the clathrin-binding and J-domain functions was expressed in *E. coli* and purified as described[16].

Bovine Hsc70 with an N-terminal histidine tag was expressed in *E. coli* strain BL21-DE3 using a pProEX HTc vector. The C terminus of Hsc70 was modified for site-specific labeling by adding a glycine and a cysteine residue (**Supplementary Fig. 5**). Affinity purification was followed by TEV protease cleavage to remove the histidine tag. Undigested fusion protein was removed by binding to cobalt beads. The C-terminal cysteine residue of Hsc70 was labeled with an excess of AF568–C5-maleimide. Labeled Hsc70 was purified by gel filtration. The labeling yield determined using UV-visible absorption spectroscopy was ~97%. Hsc70 without C-terminal cysteine did not incorporate an appreciable amount of label. Labeled Hsc70–ATP was monomeric and showed normal uncoating activity.

Coat formation. The clathrin adaptor complex AP-2 was purified from calf brain as described[16,25,26]. Fluorescent clathrin triskelions were mixed with AP-2 at a ratio of 3:1 (w/w) and dialyzed overnight at 4 °C against coat formation buffer (50 mM MES, pH 6.5, 100 mM NaCl, 2 mM EDTA, 0.5 mM DTT). Coats were isolated by high-speed centrifugation and resuspended in coat formation buffer. Coats assembled with labeled or unlabeled recombinant clathrin were indistinguishable from each other in clathrin–AP-2 composition, in appearance by electron microscopy and in their auxilin-, Hsc70- and ATP-dependent disassembly in the ensemble uncoating assay (**Supplementary Fig. 2**).

Mixed coats were assembled after combining wild-type triskelions labeled with AF488 and mutant triskelions labeled with DL649 in various molar ratios with AP-2. The composition of the resulting coats was determined in each coat by TIRF imaging from the relative intensities of AF488 and DL649.

Flow cell and microscopy. Glass coverslips were thoroughly cleaned, coated with a copolymer composed of poly-L-lysine and biotinylated PEG (PLL–PEG, Susos AG) in PBS and further modified with streptavidin. The flow cell was prepared by pressing a polydimethylsiloxane device with microfluidic channels (800 μm width, 80–100 μm height) onto the modified coverslip.

A schematic of the TIRF microscope is shown in **Supplementary Figure 4**. Images were acquired sequentially for each wavelength using exposures of 2–10 ms. The frame rate was limited to 1–2 Hz to prevent photo-cross-linking of the proteins within the coat. Prolonged exposure or imaging at higher frame rates led to loss of uncoating competence. All buffers contained the antioxidant Trolox (Calbiochem; 2 mM). An oxygen-quenching system containing protocatechuic acid and protocatechuate-3,4-dioxygenase[27] was used for imaging of DL649-labeled proteins.

Single-particle fluorescence imaging uncoating assay. The biotinylated antibody CVC.6 to LCa was immobilized on the streptavidin modified coverslip to capture fluorescent coats. Typically, between 600 to 1,400 coats bound to the surface per field of view (40 μm × 40 μm). Auxilin was added by flowing 24 μl of a solution of 0.05 mg ml^{-1} auxilin in uncoating buffer (20 mM imidazole, pH 6.8, 100 mM KCl, 2 mM MgCl$_2$) through the microfluidic channel at a flow rate of 8 μl min^{-1}. The uncoating reaction was initiated by introducing 20–30 μl of a mixture containing Hsc70–AF568 at various concentrations, 0.02 mg ml^{-1} auxilin and 2 mM ATP in uncoating buffer at a flow rate of 100 μl min^{-1} for rapid solution exchange followed by continuous flow at 10 μl min^{-1}.

Image analysis. Images were analyzed with software written in MATLAB (The MathWorks). Clathrin–AP-2 coats were detected as local maxima in an averaged fluorescence image. Overlapping objects (non-diffraction limited) were excluded from analysis. Fluorescence traces were calculated by Gaussian fitting of the signals in each channel and corrected for the local background. Fluorescence traces were sorted into classes characterized by how rapidly the clathrin signal decayed (**Supplementary Fig. 8**). Uncoating efficiency in **Figures 3, 4** and **8** is defined as the percentage of traces with a phase of rapid signal disappearance. Arrival of the uncoating reagents (defined as $t = 0$) was detected as an increase of the background fluorescence in the red channel. Accumulation times (defined as the time between arrival of the reagent and initiation of the phase of rapid signal disappearance) were determined for each trace using a step-fitting algorithm[28].

The relative intensities of the fluorophores (AF488, AF568 and DL649) were determined from the quantal photobleaching step in single-molecule photobleaching traces. The number of Hsc70 molecules bound per triskelion at the initiation of coat disassembly was determined from the ratio of the smoothed Hsc70 fluorescence intensity at the tie point at which disassembly began to the clathrin-coat fluorescence intensity before addition of uncoating reagents. Only coats that disassembled within the mean disassembly time of the entire population were used for this analysis.

Full methods. Full methods and a detailed description of the kinetic model are available in **Supplementary Methods**.

24. Jackson, A.P. & Parham, P. Structure of human clathrin light chains. Conservation of light chain polymorphism in three mammalian species. *J. Biol. Chem.* **263**, 16688–16695 (1988).
25. Boll, W. *et al.* Sequence requirements for the recognition of tyrosine-based endocytic signals by clathrin AP-2 complexes. *EMBO J.* **15**, 5789–5795 (1996).
26. Gallusser, A. & Kirchhausen, T. The beta 1 and beta 2 subunits of the AP complexes are the clathrin coat assembly components. *EMBO J.* **12**, 5237–5244 (1993).
27. Aitken, C.E., Marshall, R.A. & Puglisi, J.D. An oxygen scavenging system for improvement of dye stability in single-molecule fluorescence experiments. *Biophys. J.* **94**, 1826–1835 (2008).
28. Kerssemakers, J.W.J. *et al.* Assembly dynamics of microtubules at molecular resolution. *Nature* **442**, 709–712 (2006).